Journal of the Korean Ceramic Society
Vol. 45, No. 10, pp. 579~583, 2008.

Fabrication and Characterization of Porous TCP coated Al_2O_3 Scaffold by Polymeric Sponge Method

Swapan Kumar Sarkar, Young Hee Kim, Min Sung Kim, Young Ki Min, Hun Mo Yang, Ho-Yeon Song, and Byong-Taek Lee†

Department of Biomedical Engineering and Materials, School of Medicine, Soonchunhyang University, Chungnam 330-090, Korea
(Received September 25, 2008; Revised October 15, 2008; Accepted October 16, 2008)

ABSTRACT

A porous Al_2O_3 scaffold coated with tricalcium phosphate (TCP) was fabricated by replica method using polyurethane (PU) foam as a fugitive material. Successive coatings of Al_2O_3 and hydroxyapatite (HAp) were applied via dip coating onto polyurethane foam, which has a slender and well interconnected network. A porous structure was obtained after sequentially burning out the foam and then sintering at 1500°C. The HAp phase was changed to TCP phase at high temperature. The scaffold showed excellent interconnected porosity with pore sizes ranging from 300~700 μm in diameter. The inherent well interconnected structural feature of PU foam remained intact in the fabricated porous scaffold, where the PU foam material was entirely replaced by Al_2O_3 and TCP through a consecutive layering process. Thickness of the Al_2O_3 base and the TCP coating was about 7~10 μm each. The TCP coating was homogeneously dispersed on the surface of the Al_2O_3 scaffold.

Key words*: *TCP coating, Scaffold, Porous structure

1. Introduction

In recent decades tissue engineering has been the focus of intensive research. New approach to solve problems involved in tissue replacement or augmentation in different parts of the human body is currently being developed in this field. Replacement of hard tissue or filling empty space in bone with calcium phosphate based ceramics or bioglass has been investigated. Tissue engineering for hard tissue replacement or augmentation has opened a new frontier of research. Scaffolds for bone tissue engineering have been investigated recently.[1,2] Various synthetic alternatives such as ceramics, polymers, and composites have been evaluated as scaffolds.[3,4] With respect to the scaffold, it is generally agreed that a highly porous scaffold with interconnected pores is necessary for the easy of hard tissues in-growth.[5-7] However, unlike most other scaffolds for tissue engineering, the one used in bone tissue engineering must be mechanically strong enough to withstand the mechanical load it has to bear after implantation with out sacrificing its shape and characteristics after being embedded in the body.[8-10]

With the growing demand for employing bioactive materials for orthopedic applications as well as in maxillofacial surgery, the utilization of bioceramics such as hydroxyapatite (HAp) and tricalcium phosphate (TCP) as fillers, spacers, and bone graft substitutes has proliferated, primarily because of their biocompatibility, bioactivity, and osteoconduction characteristics with respect to bone tissue.[11-13] Recently, attempts have been taken to fabricate HAp scaffolds by replica method. However, there are critical limitations in applying these scaffolds to real system because of their lower compressive strength[14,15] Alumina ceramics have been used for implants and prostheses during the past several decades.[16] The material is characterized by its excellent biocompatibility,[17] as well as its high strength, hardness and fracture resistance.[18,19] High purity alumina bioceramics have been developed as an alternative to surgical metal alloys for total hip prosthesis and tooth implants.[20] As such, integrating of the bioactivity of TCP and the mechanical strength of Al_2O_3 could fulfill the bioactivity and mechanical strength requirement in a new scaffold design for tissue engineering.

In this work, a highly porous TCP coated Al_2O_3 body with interconnected porosity was fabricated by a replica method using polyurethane foam.

2. Experimental Procedure

The porous scaffold was made by a previously reported polyurethane foam replica method.[21] The coating slurry was prepared from Al_2O_3 (AKP 50, sumitomo, Japan) and HAp powder which was synthesized in our laboratory by a microwave-hydrothermal method[22] 50 g of Al_2O_3 powder was stirred vigorously in 100 ml distilled water for 4h. As a binder, 5 g poly vinyl butyl (PEG, Duksan Pure Chemical Co. Ltd, Korea) was dissolved in another beaker for 1 h, and was subsequently added to the slurry and stirred for an

†Corresponding author : Byong-Taek Lee
E-mail : lbt@sch.ac.kr
Tel : +82-41-570-2427 Fax : +82-41-577-2415

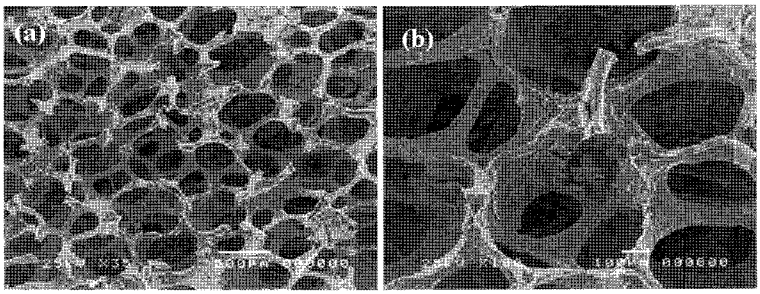

Fig. 1. SEM micrographs of TCP coated Al_2O_3 scaffold (a) low magnification and (b) enlarged image.

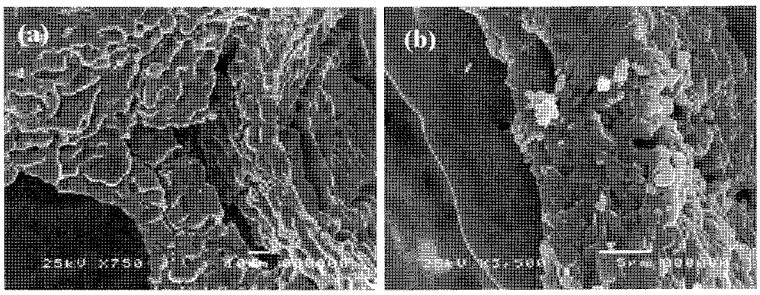

Fig. 2. SEM micrographs of TCP coated Al_2O_3 scaffold (a) surface coating on pore frame and (b) cross sectional view.

additional 24 h. Polyurethane foam templates (Customs Foam Ltd., UK) cut to appropriate dimensions was immersed in the slurry. After blowing with an air gun to disperse the slurry uniformly throughout the porous scaffolds without blocking the pores, the sponge was dried at 80°C for 8 h. These dipping-and-drying steps were repeated three times. HAp slurry was made in the same procedure as noted above and a HAp slurry coating was applied onto the dried Al_2O_3 coating following the same process. Application of the HAp slurry was performed three times to ensure a homogenous coating. The obtained green body was heat-treated to burn out the sponge and binder at 600°C for 3 h at a heating rate of 1°C/min. Subsequent sintering of the porous body was performed at 1500°C at a heating rate of 5°C/min for 2 h holding time.

The relative density of the porous scaffold was measured by the Archimedes method. The pore size and microstructure of the porous scaffold were investigated by scanning electron microscopy (SEM, JSM-635F, Jeol). To identify the crystal structure and phases, an X-ray diffractometer (XRD, D/MAX-250, Rigaku, Japan) was used. Specimens with dimensions of $12\times8\times8$ mm^3 were used for a compression test using a universal testing machine (UnitechTM, R&B, Korea) with a crosshead speed of 0.5 mm/min in ambient conditions. The stress-strain curve obtained was used to determine mechanical properties. The compressive strength was determined from the maximum load recorded and from the slope at the initial stage, respectively. Five specimens were tested for each condition.

3. Results and Discussion

Fig. 1 showed SEM micrographs of the porous scaffold, (a) low magnification and (b) enlarged image. These figures revealed that the structure of the obtained scaffold is similar to classic cancellous bone having a three-dimensional open cellular morphology. The pore sizes were about 100~600 μm and were highly homogeneous throughout the scaffold. All the porous spaces were interconnected to each other. The frame of the scaffold was thin enough that it occupied a smaller portion of the scaffold volume than the porous space. Consequently, the porosity of the fabricated scaffold was very high. This higher porosity level and suitable pore size are critical to the proliferation of the growing hard tissue during tissue culture and after implantation[23] From the enlarged image 1(b), numerous cracks and fissures which originated during the sintering process, can be observed. These cracks are attributed to the ceramic slurry coating not being dense enough to retain its integrity. This was exacerbated by the fact that the supporting PU foam was burnt out at the pre-sintering burn out phase thus leaving a hollow space there. While such cracks and flaws are inevitable they are a noteworthy hindrance to the improvement of the mechanical properties. Furthermore, the thermal expansion coefficient of Al_2O_3 and TCP differs to a considerable extent. This has a detrimental effect on the morphology of the TCP coating as this upper coating expands and contracts almost three times more intensely than the Al_2O_3 phase.

Fig. 2 (a) showes the TCP coating on the frame. The TCP phase was melted at 1500°C and covered the entire surface of the Al_2O_3. The surface was highly rough. Surface roughness is especially beneficial for improved cell attachment. A rougher surface increases the surface area which translates to a quicker resorption rate of the coating and faster ossification. Some cracks were observed as discussed in relation

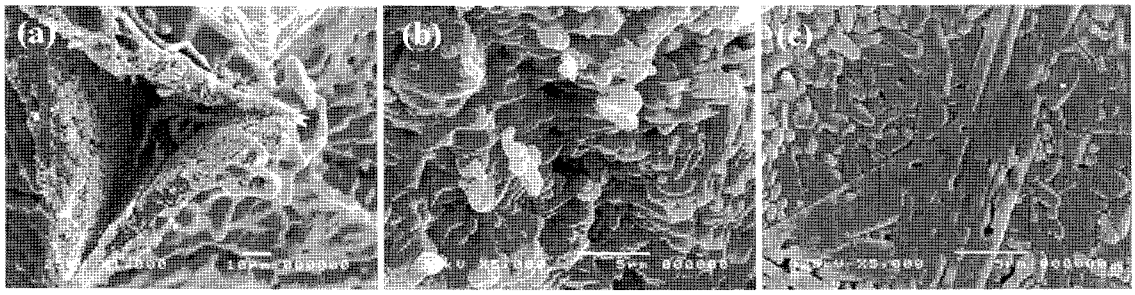

Fig. 3. SEM micrographs of TCP coated Al_2O_3 scaffold (a) cross sectional view of frame, (b) internal pore surface, and (c) Al_2O_3 phase of the frame.

to the previous figure. The enlarged SEM image in Fig. 2(b) shows a cross section of the TCP coating on the Al_2O_3 base. The TCP coating was 7 ~ 10 μm in thickness and covered the Al_2O_3 phase uniformly. The Al_2O_3 base was well densified.

During the burning out process the PU foam was removed completely and the space it previously occupied remained as a hollow space. As the entire Al_2O_3 base coat was applied onto the surface of the PU foam, the hollow region remained throughout scaffold. This hollow space is presumably interconnected as the PU frame was continuous. This rendered the fabricated porous scaffold a bimodal porosity, the original porous space from the PU foam and another porous region originating from the elimination of the PU frame itself. This internal porosity is clearly evident from Fig. 3 (a). The internal frame porosity showed distinguished size depending on the dimensions of the interconnected fibrous frame of the original PU foam. Fig. 3(b) shows the Al_2O_3 surface of the internal pore space; this surface is also very rough. Fig. 3(c) shows an enlarged SEM image of the Al_2O_3 base frame. It can be seen that some elongated grains appeared due to the presence of HAp at high sintering temperature. Beyond 1200°C, HAp starts degrading to TCP, as delineated in the following reaction

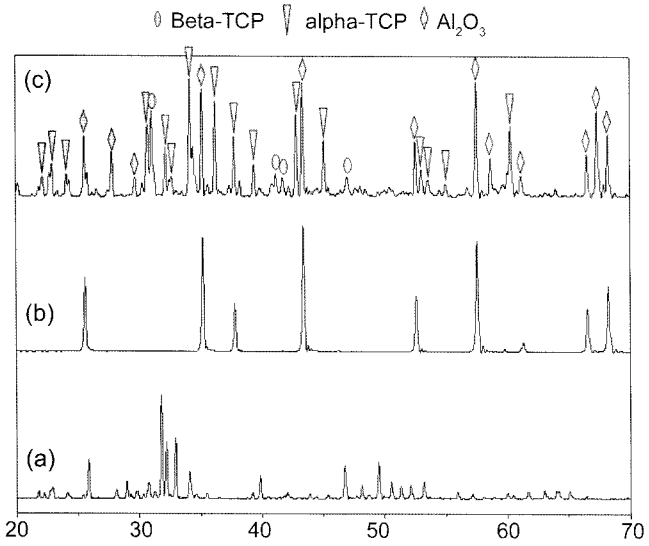

Fig. 4. XRD profiles of (a) HAp powder, (b) Al_2O_3 powder, and (c) TCP coated Al_2O_3 scaffold.

$$Ca_{10}(PO_4)_6(OH)_2 \rightarrow 3Ca_3(PO_4)_2 + CaO + H_2O$$

The CaO at high temperature reacts with the Al_2O_3 phase and causes grain elongation.[24] However, elongated grains have been reported to improve the mechanical properties to a small extent, which may prove beneficial in this type of composite scaffold.

Fig. 4 shows XRD profiles of the (a) HAp and (b) Al_2O_3 raw powder and (c) sintered porous scaffold. The XRD profile (c) reveals that all the HAp phase was converted to TCP phase. Both α-TCP and β-TCP phase were detected in the scaffold.

Fig. 5 shows the in-vitro investigation results for the fabricated scaffold and a comparison was made with the results for uncoated Al_2O_3 porous body. Cellular attachment and proliferation of MG-63 cells under static seeding on both Al_2O_3 and TCP coated Al_2O_3 porous scaffold are shown. After 3 days of cell seeding the cells were spread in both scaffolds. However, in the TCP coated Al_2O_3, the cell proliferation was evidently better with development of lamellopodia and excellent attachment with the scaffold surface could be observed. In the case of the TCP coated Al_2O_3 scaffold, after 14 days of seeding, cells were well grown and had spread uniformly and extensively, covering the surfaces of the biomaterials. The cellular morphology showed that the cell adhesion was very good with the presence of lamellapodia and an interlaced fibrous network. On the contrary, the cellular morphology on the Al_2O_3 scaffold revealed that the cell spreading was not sufficiently extensive and needle shape cells were observed and less surface space was covered after 2 weeks of cell seeding. Filopodia activity was minimal in this case. Thus there is a clear distinction between the bioactivity of these two kinds of scaffolds.

Table 1 presents the relative density and compressive strength of both of the porous scaffolds. The relative density for both of the scaffolds was around 13%, indicating that the scaffolds have a very high extent of porosity. The compressive strength was much higher in the case of the Al_2O_3 scaffold, thus again validating the usability of this material in the scaffold system. However, the scaffold did not show a reasonable value of compressive strength as expected. The large variance in the thermal expansion coefficient degraded the microstructure and consequently affected the mechanical strength as well. However, design changes to

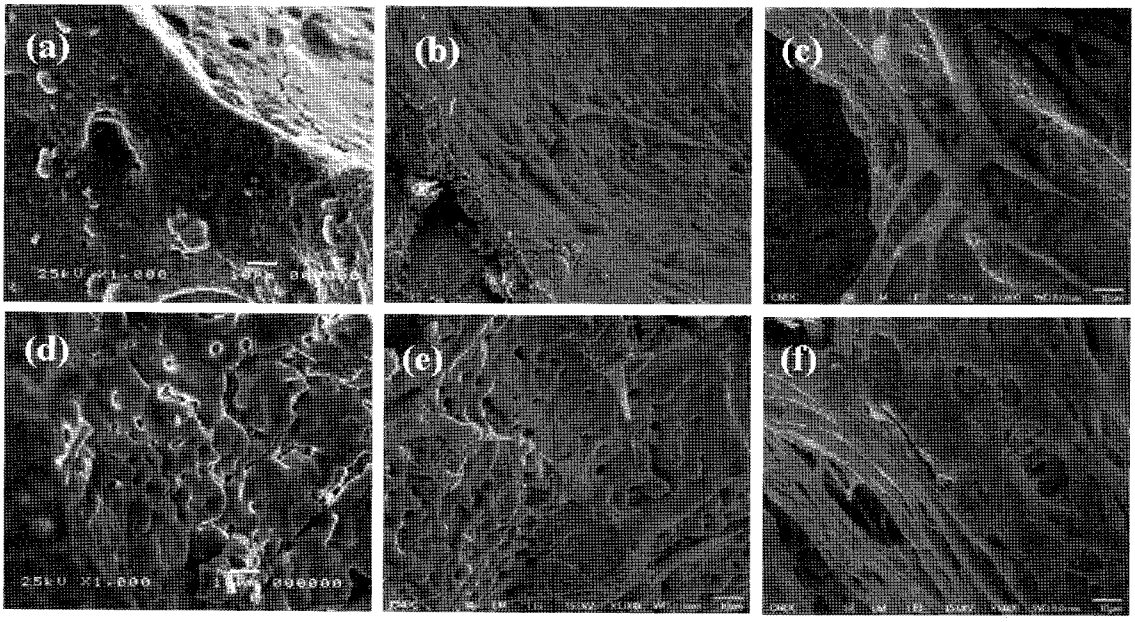

Fig. 5. SEM images of the Scaffold surface with static seeding. Al_2O_3 scaffold without seeding (a), after 3 days (b), and 14 days of seeding (c). TCP coated Al_2O_3 scaffold without seeding (d), after 3 days (e), and 14 days of seeding (f).

Table 1. Relative Density and Compressive Strength of the Monolithic Al_2O_3 Porous Scaffold and the TCP Coated Al_2O_3 Porous Scaffold

Material Properties	Al_2O_3 scaffold	TCP coated Al_2O_3 scaffold
Relative density (%)	13.03	13.00
Compressive strength (Mpa)	3.15	0.62

address the difference in the thermal expansion coefficient and can lead to with the realization of a highly bioactive and mechanically stable scaffold, starting from the same basic scaffold design.

4. Conclusion

In this study a TCP coated Al_2O_3 porous scaffold was successfully fabricated by a replica method with dip coating. The porosity was well developed and interconnected, thereby facilitating cell proliferation. The TCP coating was well furnished on-to the base Al_2O_3 coating and the coating remained intact without any sign of de-bonding or exfoliation, although some cracks were visible. Invitro investigation revealed that the TCP coated Al_2O_3 scaffold had very good cell adhesion and proliferation behavior.

Acknowledgment

This research was supported by a grant from the Center for Advanced Materials Processing (CAMP) of the 21st Century Frontier R&D Program funded by the Ministry of Commerce, Industry and Energy (MOCIE), Republic of Korea.

REFERENCES

1. Y. Yan, X. Zhuo, and Y. Hu, "Layered Manufacturing of Tissue Engineering Scaffolds Via Multi-nozzle Deposition," *Mater. Lett.*, **57** 2623-28 (2003).
2. V. Sikavitsas, G. Bancroft, Mikos, "Formation of Three-dimensional Cell/polymer Constructs for Bone Tissue Engineering in a Spinner Flask and a Rotating Wall Vessel Bioreactor," *J. Biomed. Mater. Res.*, **62** 136-48 (2002).
3. G.T. Kose and H. Kenar, "Macroporous Poly(3-hydroxybutyrate-co-3-hydroxyvalerate) Matrices for Bone Tissue Engineering," *Biomaterials*, **24** 1949-58 (2003).
4. J.P. Vacanti, C.A. Vacanti, R. Langer, "Principles of Tissue Engineering," p. 1, Academic Press, San Diego, 1997.
5. S.L. Ishaug, G.M. Crane, M.J. Miller, A.W. Yasko, M.J. Yazemski, and A.G. Mikos, "Bone Formation by Three-dimensional Stromal Osteoblast Culture in Biodegradable Polymer Scaffolds," *J. Biomed. Mater. Res.*, **36** 17-28 (1997).
6. H. Yoshimoto, Y.M. Shin, H. Terai, and J.P. Vacanti, "A Biodegradable Nanofiber Scaffold by Electrospinning and its Potential for Bone Tissue Engineering," *Biomaterials*, **24** 2077-82 (2003).
7. Y. Hu, D.W. Grainger, S.R. Winn, and J.O. Hollinger, "Fabrication of Poly(-hydroxy acid) foam Scaffolds Using Multiple Solvent Systems," *J. Biomed. Mater. Res.*, **59** 563-72 (2001).
8. T. Nezu, F.M. Winnik, "Interaction of Water-soluble Collagen with Poly(acrylic acid)," *Biomaterials*, **21** 415-19 (2000).
9. L. Huang, K. Nagapaudi, R.P. Apkarian, and E.L. Chaikof, "Engineered Collagen-PEO Nanofibers and Fabrics," *J. Biomater. Sci. Polym. Ed.*, **12** 979-93 (2001).
10. A.S. Goldstein, G. Zhu, G.E. Morris, R.K. Meslenyi, and A.G. Mikos, "Effect of Osteoblastic Culture Conditions on

the Structure of Poly(DL-Lactic-co-Glycolic Acid) Foam Scaffolds," *Tissue Eng.*, **5** 421-33 (1999).
11. K. D. Groot, "Bioceramics Consisting of Calcium Phosphate Salts," *Biomaterials*, **1** 47-50 (1980).
12. M. Jarcho, "Calcium Phosphate as a Hard Tissue Prosthetics," *Clin. Orthop. Rel. Res.*, **157** 259-78 (1981).
13. C. J. Damien and J. R. Parsons, "Bone Graft and Bone Graft Substitutes: A Review of Current Technology and Applications," *J. Appl. Biomaterials*, **2** 187-208 (1990).
14. H. W. Kim, S. Y. Lee, C. J. Bae, Y. J. Noh, H. E. Kim, H. M. Kim, and J. S. Ko, "Porous ZrO_2 Bone Scaffold Coated with Hydroxyapatite with Fluorapatite Intermediate Layer," *Biomaterials*, **24** 3277-82 (2003).
15. H.W. Kim, J.C. Knowles, and H.E. Kim, "Hydroxyapatite/poly(ε-caprolactone) Composite Coatings on Hydroxyapatite Porous Bone Scaffold for Drug Delivery," *Biomaterials*, **25** 1279-87 (2004).
16. S. F. Hulbert, F. A. Young, R. S. Mathews, J. J. Klawitter, C. D. Talbert, and F. H. Stelling, "Potential of Ceramic Materials as Permanently Implantable Skeletal Prostheses," *J. Biomed Mater. Res.*, **4** 433-56 (1970).
17. P. Griss and E. Werner, "Mechanical Properties of Biomaterials," p. 217, Wiley, London, 1980.
18. D. J. Green., "An Introduction to the Mechanical Properties of Ceramics," Cambridge University Press; Cambridge, 1998.
19. D. Munz and T. Fett, "Ceramics: Mechanical Properties, Failure Behaviour, Materials Selection, 1st ed," *Springer*, Berlin, Heidelberg, New York, 1999.
20. H. Fischer, C. Niedhart, N. Kaltenborn, A. Prange, R. Marx, F. U. Niethard, and R. Telle, "Bioactivation of Inert Alumina Ceramics by Hydroxylation," *Biomaterials*, **26** 6151-57 (2005).
21. E.A. Moreira, M.D.M. Innocentini, and J.R. Coury, "Permeability of Ceramic Foams to Compressible and Incompressible Flow," *J. Euro. Ceram. Soc.*, **24** 3209-18 (2004).
22. J.K. Han, H.Y. Song, F. Saito, B.T. Lee, "Synthesis of High Purity Nano-sized Hydroxyapatite Powder by Microwave-hydrothermal Method," *Mater. Chem. Phy.*, **99** 235-39 (2006).
23. L. Cerroni, R. Filocamo, M. Fabbri, C. Piconi, S. Caropreso, S.G. Condo, "Growth of Osteoblast-like Cells on Porous Hydroxyapatite Ceramics: an in Vitro Study," *Biomolecular Engineering*, **19** 119-24 (2002).
24. W.A. Kaysser, M.Sprissler, C.A. Handwerker, J.E. Blendelll, "Effect of a Liquid Phase on the Morphology of Grain Growth in Alumina," *J. Am. Ceram. Soc.*, **70** [5] 339-43 (1987).